The Journal of Adhesion, 87:1059–1072, 2011

ISSN: 0021-8464 print/1545-5823 online
DOI: 10.1080/00218464.2011.609439

Taylor & Francis
Taylor & Francis Group

Normal Adhesive Force-Displacement Curves of Living Geckos

N. Pugno[1,2,3], E. Lepore[1], S. Toscano[4], and F. Pugno[1]
[1]Laboratory of Bio-inspired Nanomechanics "Giuseppe Maria Pugno," Department of Structural Engineering and Geotechnics, Politecnico di Torino, Torino, Italy
[2]National Institute of Nuclear Physics, National Laboratories of Frascati, Frascati, Italy
[3]National Institute of Metrological Research, Torino, Italy
[4]DVM, Torino, Italy

In this paper, we report experimental measurements of normal adhesive force versus *body displacement for living Tokay geckos (*Gekko gecko*) adhered to Poly(methyl meth acrylate) (PMMA) or glass surfaces. We have measured the normal adhesive force needed for reaching the gecko detachment. Atomic force and scanning electron microscopies are used to characterize the surfaces and feet topologies. The measured safety factors (maximum adhesive force divided by the body weight) are 10.23 on PMMA surfaces or 9.13 on glass surfaces. We have observed minor and reversible damage of the gecko feet caused by our tests, as well as the self-renewal of the gecko adhesive abilities after the moult.*

Keywords: Adhesion; Force; Geckos; Living; Safety factor

1. INTRODUCTION

The ability of a gecko to stay stuck motionless to a vertical surface or even to a ceiling seems to defy gravity. Since the 4th century B.C. geckos have been observed to "run up and down a tree in any way, even with their head downwards [1]" by Aristotle. Scientific researchers have focused their attention on the gecko adhesive foot

Received 9 November 2010; in final form 20 April 2011.
Address correspondence to N. Pugno, Laboratory of Bio-inspired Nanomechanics "Giuseppe Maria Pugno," Department of Structural Engineering and Geotechnics, Politecnico di Torino, Corso Duca degli Abruzzi, 24, 10129 Torino, Italy. E-mail: nicola.pugno@polito.it

architecture, adhesion abilities, and related mechanisms [2–20]. Scanning electron microscopy (SEM) has brought about new opportunities to go under the length-scale limitations given by the wavelength of visible light and to study the sub-micrometric hierarchical architecture of gecko's toes.

The Tokay gecko (*Gekko gecko*) is the second largest Gekkonid lizard species (1050 species in the world), attaining lengths of approximately 0.3–0.4 m or 0.2–0.3 m for males or females, respectively. The weight of an adult gecko ranges from $\sim$30 up to $\sim$300 g [21]. A previous study on Tokay geckos [2] revealed a strong shear adhesive force of $\sim$20 N when placed with its front feet contacting a nearly vertical (85°) acetate sheet attached to a stiff PMMA plate. As a consequence, if we assume a gecko weight of $\sim$100 g, we estimate a shear safety factor (SF) of approximately 40. This SF is comparable with that of the *Hemisphaerota cyanea* beetle (SF $\sim$ 60; measured for a force applied perpendicularly to the vertically-oriented attachment surface; generated either electronically or by hanging weights [22]), of the *Chrysolina Polita* leaf beetle (SF $\sim$ 50; attached to a force transducer [17]), but lower than the SF of the jumping spider *Evarcha arcuata* (SF $\sim$ 160; theoretically extracted *via* atomic force microscopy (AFM) analysis [23]) and of *Crematogaster* cocktail ants (SF $\sim$ 146; measured using a centrifuge technique [24]). Thus, not only for insects and spiders [2,17,22–25], but also for geckos, several studies have been carried out with the aim of quantifying the maximal adhesive force by direct *in vivo* [2,19,26–33] or *in vitro* measurements [19,26–30].

In this paper, we report measurements of the normal adhesive force *versus* body displacement of living Tokay geckos, up to the detachment. We are also interested in comparing the effects of surface roughness on the gecko maximum normal safety factor. The influence of the damage of the gecko's feet, caused by our experimental tests, on the adhesive abilities is also discussed. The surface topography of PMMA or glass was analyzed by AFM, whereas we have used SEM to characterize the hierarchical architecture of the gecko's feet.

2. MATERIALS AND METHODS

2.1. PMMA and Glass Surface Characterization

The roughness of the adhering surfaces, PMMA and glass, was nano-characterized by AFM Perception (Assing, Rome, Italy) using the contact mode with a silicon nitride tip. A surface area of $10 \times 10\,\mu m^2$ for each material was evaluated with a final resolution of 200

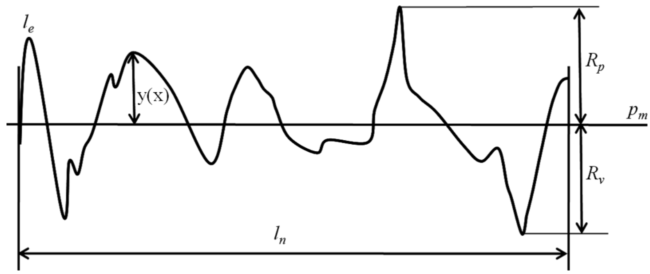

FIGURE 1 General scheme of a profile for the definition of the roughness parameters.

points/profile. The roughness parameters of interest were: the standard amplitude parameters R_a, R_q, R_p, R_v, and S_{sk} and the hybrid parameters S_{dr} (for details, see Fig. 1). R_a represents the arithmetical average roughness ($R_a = \frac{1}{l_n}\int_0^{l_n} |y(x)|dx$); R_q is the mean square roughness and represents the mean square deviation of the profile from the middle line ($R_a = \sqrt{\frac{1}{l_n}\int_0^{l_n} y^2(x)dx}$); R_p and R_v are, respectively, the height of the highest peak and the depth of the deepest valley (absolute values). The parameters S_{Sk} and S_{dr} offer a comprehensive overview of the surface's characteristics, indicating, respectively, the surface skewness and the surface complexity. When S_{Sk} is close to 0, the surface is equally distributed on the middle plane (p_m), when lower than 0 the surface is characterized by plateaus and several deep thin valleys, whereas when higher than 0 the surface is characterized by plateaus and several peaks. The parameter S_{dr} compares the effective surface (l_e) with the nominal one (l_n): when close to 0%, the surface is smooth, when higher the surface is characterized by a specific superficial complexity.

2.2. Gecko Normal Adhesive Force *versus* Displacement Curves

We used a single male adult Tokay gecko (authorized by Ministerial Decree n° 73/2010-B). The gecko was maintained in its terrarium at ~28°C. The temperature of the experimental room, in which the force-displacement measurements were made, was ~22°C. The gecko was fed moths and water *ad libitum* and crickets one time a week. The animal did not show any particular discomfort being manipulated, segregated in the box, and bound with adherent elastic cloth bandaging.

Force-displacement measurements were conducted as follows. The gecko was prepared and placed in the PMMA-Glass (Vetronova, Varese, Italy) box 10 minutes before each set of tests. We took the gecko from its terrarium and we fixed to it an adherent cloth bandaging; a metallic hook was inserted within the bandage on the gecko's back. After this preliminary operation, the gecko was connected, by means of a plastic wire tied to the metallic hook, to the measurement platform, and it was placed gently on the bottom of the measurement box (Fig. 2). The force-displacement measurement platform was built outside the box (Fig. 3) We applied the force using an increasing amount of mass (16, 48, 98, 148, 198, 273, 348, 423, 498, 573, 648, and 723 g). The displacements of the point of applied force on the gecko body were recorded during the test. The measured displacement corresponds to the stretching of the front and rear legs of the gecko without slipping of its feet.

The procedure of increasing hung weights was conducted as follows. We started with the application of 16 g. We waited 10 seconds for a stabilized value of the gecko displacement and read it on a millimetric scale. Similarly, we continued with the next applied weights up to 198 g. For larger weights we allowed a relaxing time of about 15 s after each weight application to try to avoid the gecko muscular fatigue. When the detachment occurred, the gecko was pulled upwards but immediately reached a secure point, approximately 42 cm from the top of the box and then was slowly taken back to the bottom. Each

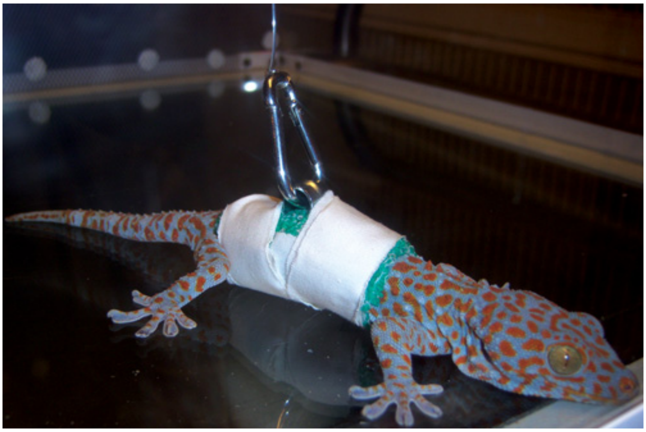

FIGURE 2 Our tested Tokay gecko: adherent elastic cloth bandaging and metallic hook of connection with the outside measurement platform (color figure available in online).

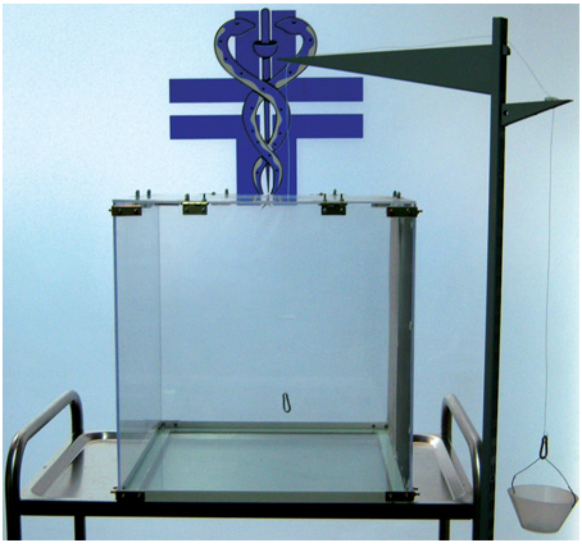

FIGURE 3 Force-displacement measurement platform (color figure available in online).

force-displacement curve was obtained in ~3 minutes. During a single test, the only allowed action was the renewal of the foot contact and hyperextension [2].

We have accordingly measured the normal adhesive force-displacement curves of a gecko adhered to the interior surface of a box ($50 \times 50 \times 50\,\text{cm}^3$). One wall of the box was made of glass and the other walls were made in PMMA. We realized 15 tests on PMMA and three tests on glass after a first moulting process (first moult) and three tests on PMMA and four tests on glass after the next moulting (second moult).

After the first moult, in the first test-day that was 50 days from the moult, we realized only one force-displacement curve, both on PMMA and glass (blue line, Figs. 4 and 5 respectively). After 62 days from the moult, we performed the second day of tests: we carried out four tests on PMMA (cyan line, Fig. 4) and two tests on glass (cyan line, Fig. 5). The third test-day took place the day after and we realized 10 tests on PMMA (green line, Fig. 4). After the second moult, we only conducted experiments on one day, 7 days after moult, due to the damage imposed by this first day of tests on the gecko's feet. We started on glass, performing four tests (red line, Fig. 5), and then on PMMA measuring three force-displacement curves (red line, Fig. 4).

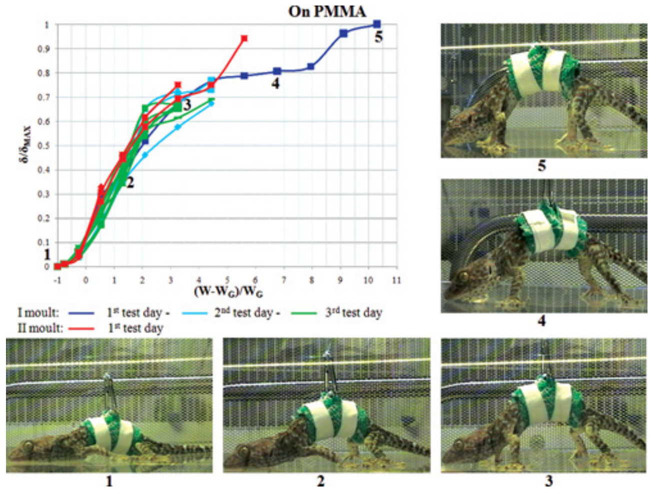

FIGURE 4 Normal adhesive force-displacement curves on PMMA surfaces after the first and second moults. Snapshots show five specific instants of the gecko displacement at 0, 148, 273, 423, and 723 g of hung weight (W is the applied weight, W_G is the gecko weight, δ is the gecko displacement, δ_{MAX} is the gecko maximum displacement) (color figure available in online).

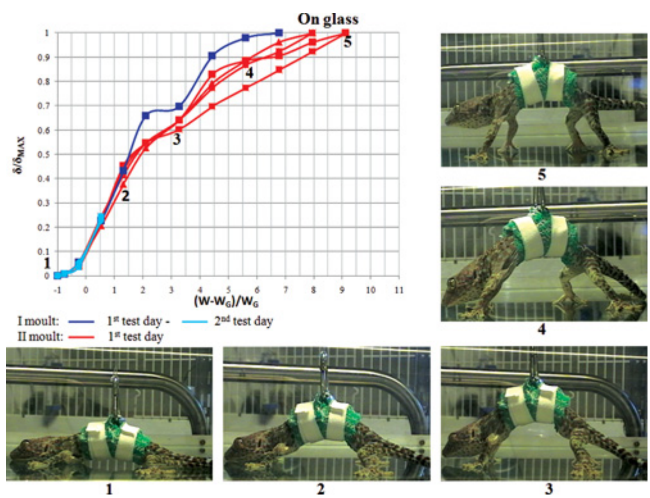

FIGURE 5 Normal adhesive force-displacement curves on glass surface after the first and second moults. Snapshots show five specific instants of the gecko displacement at 0, 148, 348, 423, and 648 g of hung weight (W is the applied weight, W_G is the gecko weight, δ is the gecko displacement, δ_{MAX} is the gecko maximum displacement) (color figure available in online).

3. RESULTS

3.1. Gecko's Feet Architecture

The Tokay gecko foot consists of five digits (Fig. 6A) covered with macroscopic hairy structures called lamellae (~0.5–3 mm in width and 200–500μm in length, Fig. 6B). These lamellae are organized in a series of multi-arrays localized perpendicular to the longitudinal axis of each digit; the lamellae are separated one from another. Nanostructured hairy units ~2–5 μm in length and ~200 nm in diameter, Figs. 6C, 6D) have been identified on the connection areas between adjacent lamellae (Fig. 6C) and on the edge of each single digit (Figs. 7B, C, D). Each lamella is covered with several thousand setae (10–130 μm in length and 3–10 μm in diameter, density of ~0.014 setae/μm^2 [12,34], Figs. 8B, 8C), which in turn contain at their tips hierarchical substructures called spatulae (0.1–0.2 μm wide and 15–20 nm thick, Figure 8D). Terminal claws are located at the top of each single toe (~500 μm in diameter and ~1 mm in length, Fig. 6A) and guarantee a secure mechanical interlocking on surfaces with high roughness, *i.e.*, where the diameter of the gecko's claw tip is smaller than the roughness [35–40].

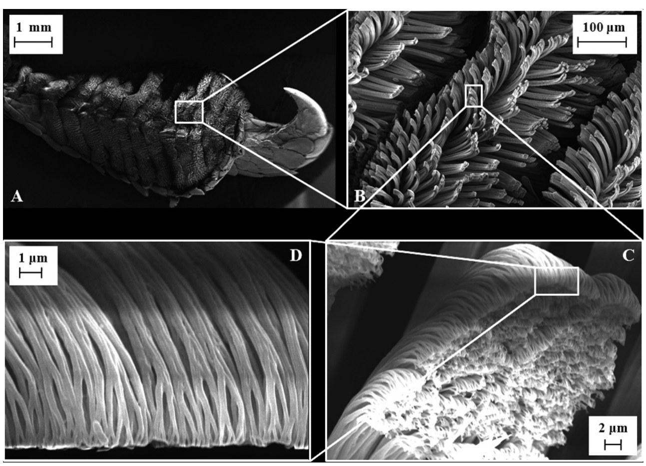

FIGURE 6 (A, B) Tokay gecko adhesion system observed by FESEM (ZEISS SUPRA 40) and (C, D) by SEM (ZEISS EVO 50) (A) Toe and FESEM micrograph of the (B) setae. (C) SEM micrograph of the setae and (D) a nanoscale array of hundreds of spatule.

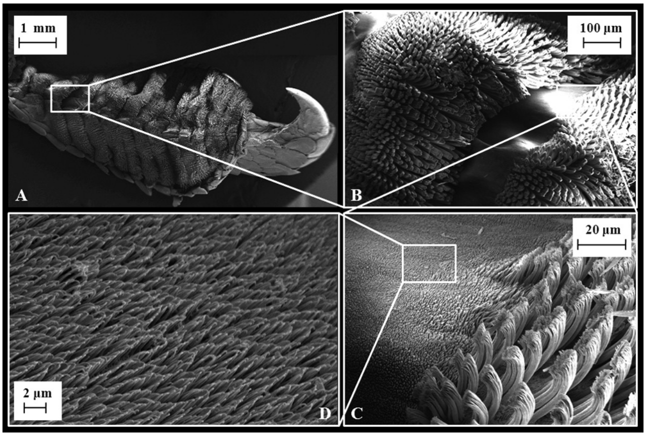

FIGURE 7 Tokay gecko adhesion system observed by FESEM (ZEISS SUPRA 40). (A) Tokay gecko toe. (B, C) The connection area between adjacent lamellae, that are localized perpendicular to the longitudinal axis of each digit, is covered by nanostructured hairy units; (D) at high magnification.

3.2. PMMA and Glass Surface Characterization

Table 1 summarizes roughness parameters of the considered PMMA and glass surfaces. The PMMA (Fig. 9) and glass (Fig. 10) surfaces

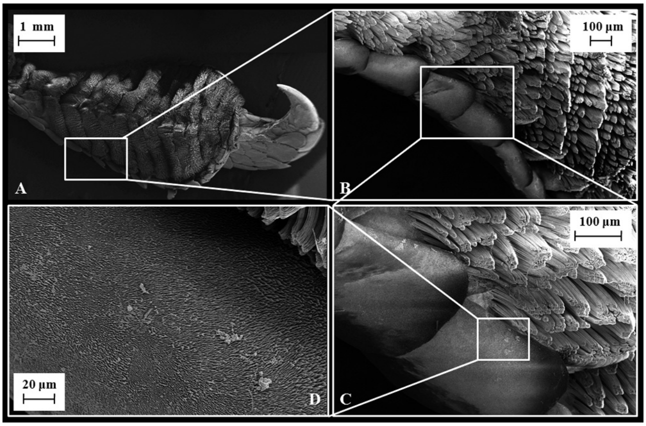

FIGURE 8 Tokay gecko adhesion system observed by FESEM (ZEISS SUPRA 40). (A) Tokay gecko toe. (B, C) The edge of the gecko toe is covered by nanostructured hairy units; (D) at high magnification.

TABLE 1 Roughness Parameters of the Considered PMMA or Glass Surfaces

	PMMA	Glass
Ra [nm]	3.8 ± 0.085	0.80 ± 0.214
Rq [nm]	5.88 ± 0.778	1.4 ± 0.796
Rv [nm]	52.74 ± 14.938	16.88 ± 13.895
Rp [nm]	90.06 ± 28.736	21.6 ± 16.943
Ssk	1.4 ± 0.997	0.79 ± 0.461
Sdr (%)	0.60 ± 0.046	0.02 ± 0.007

are different in terms of roughness. In addition, on the glass surface isolated bubbles of $\sim$1 μm in diameter are recognizable.

3.3. Gecko Normal Adhesive Force *versus* Displacement Curves

After the first moult on the PMMA surface, we obtained a maximum SF $\lambda_{\text{PMMA(I)-1Day}} = 10.23$ in the first test-day. Note that to compute this value we have considered the measured animal weight (64 g) and the final hung weight of 723 g (Fig. 4, snapshot 5). In the second test-day, the gecko reached an average SF reduced by 60% ($\lambda_{\text{PMMA(I)-2Day}} \approx 4.1$), in comparison with the maximum value. Finally, the SF reached a minimum value equal to $\lambda_{\text{PMMA(I)-3Day}} \approx 2.1$ during the third test-day. Analogously, on the glass surface, the final hung weight of 498 g and the same gecko weight correspond to a maximum SF $\lambda_{\text{Glass(I)-1Day}} \approx 6.8$ in the first test-day. In the second test-day, it is reduced to less than 1 ($\lambda_{\text{Glass(I)-2Day}} \approx 0.5$). In the first test-day after the second moult, the final maximum hung weight of 648 g and the same gecko weight correspond to a maximum SF $\lambda_{\text{Glass(II)-1Day}} = 9.13$ (Fig. 5, snapshot 5). After four

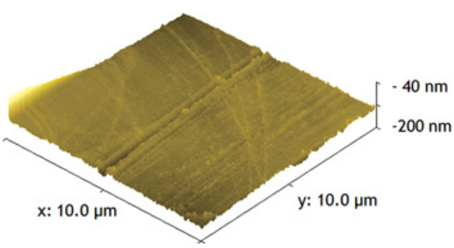

FIGURE 9 AFM characterization of the PMMA surface (color figure available in online).

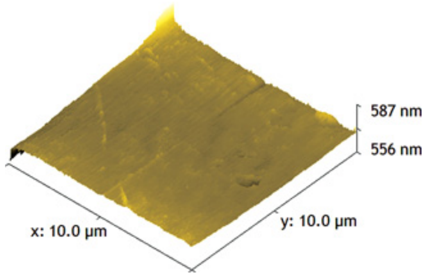

FIGURE 10 AFM characterization of the glass surface (color figure available in online).

tests on the glass surface, we performed three tests on the PMMA surface, reaching a SF that gradually decreases starting from a value $\lambda_{\mathrm{PMMA(II)\text{-}1Day}} \approx 5.6$ up to a final minimum value $\lambda_{\mathrm{PMMA(II)\text{-}1Day}} \approx 0.5$. In summary, the final maximum SF is found to be $\lambda_{\mathrm{PMMA}} = \lambda_{\mathrm{PMMA(I)\text{-}1\,Day}} = 10.23$ on the PMMA surface and $\lambda_{\mathrm{Glass}} = \lambda_{\mathrm{Glass(II)\text{-}1Day}} = 9.13$ on the glass surface.

4. DISCUSSION

Figures 4 and 5 report our results of force-displacement curves and five snapshots of specific gecko configurations on PMMA or glass, respectively. We condensed all the obtained force-displacement curves, measured during the best gecko condition (first test-day after moulting) and in the course of the period after the gecko's moult (second and third test-day). In the first test-day after the first moult, we found the gecko maximum SF on the PMMA surface, while in the first test-day after the second moult, the maximum SF on the glass surface was found. The SF of ~10 that we measured for Tokay geckos is coherent with previous observations. In particular, in [2], the shear adhesive force was measured. Each gecko was gently placed with its front feet contacting a nearly vertical acetate sheet (85°) and then slowly pulled in a downward direction. Our experimental set, instead, permitted us to evaluate the normal force to detach the Tokay gecko from a horizontal surface (PMMA and glass). Thus, the maximal shear force can be estimated to be ~40 N for the living Tokay gecko [2] and now we have calculated the maximal normal adhesive force equal to 7.1 N on PMMA and 6.4 N on glass.

Considering a setae density of 14,000 setae/mm^2 [27,28,34] and a total gecko pad area of 450 mm^2, the shear adhesive force of ~40 N [2], as well as our normal adhesive force of ~6.7 N, imply for a single seta a shear adhesive force equal to 6.2 μN [28] and a normal adhesive force equal to 1.1 μN. These top-down computations are underestimated, due to the unavoidable presence of defects at the macroscale of the pads. Indeed, the maximum shear adhesive force of a single seta was directly measured as equal to ~200 μN [19,28,31], leading to a theoretical shear adhesive force for the gecko of 1250 N [28]; similarly, the maximum normal adhesive force of a single seta is ~40 μN [27,31], leading to a theoretical normal adhesive force for the gecko of 250 N [28]. At the size of the spatulae, only the normal adhesive force has been determined, equal to ~10 nN [29,30,32], which leads to a final adhesive force for a gecko of 65 N (if we consider that a gecko has 6.5 billions of spatulae [2,28,34]).

From the results at different characteristic sizes, we should conclude that the force estimated at the macroscale (*i.e.*, of the whole gecko) leads to an underestimation of nearly 32 times the microscale (setae) shear adhesive force and of nearly 36 times the microscale normal adhesive force; thus, "smaller is stronger" [41,42]. Similarly, at the nanoscale (spatulae) the normal adhesive strength is nearly 10 times the macroscale [43]. As a consequence of the presence of defects [26,31] at the level of the entire body, a normal safety factor of ~10 has to be expected, in order to have a safe attachment and an easy detachment, as we have measured.

Summarizing, the shear adhesive force is equal to ~200μN [19,28,31] for a single seta and ~40 N [2] for the whole gecko, while the normal adhesive force is equal to ~10 nN [29,30,32] for a single spatula, ~40 μm [27,31] for a single seta, and ~7.1 (~6.4) N on PMMA (glass) for the whole gecko, as here determined. Thus, our result of the normal adhesive force for the whole gecko gives a contribution to the characterization of the functionality of the hierarchical adhesive system of the Tokay gecko [44] and confirms the ratio of 5:1 between the shear and normal adhesive forces for the whole animal, as observed by Autumn *et al.* [33] for a different climbing gecko (*Hemidactylus garnotii*, ~2 g of body mass); interestingly, note that, for Tokay gecko, such a ratio of 5:1 of the shear to normal adhesive forces is verified both at macro and micro scales.

In addition, we observed the self-renewal of the gecko adhesive system after the gecko's moulting process and a negative effect of the previously executed experimental tests, leading to a reduction of the maximal adhesive force.

4.1. Feet damage

During the first test-day after the second moult, we observed evident feet damage. As mentioned above, we started by performing four tests on the glass surface and then on the PMMA surface we performed three tests, which showed that the gecko detachment force drastically decreases from one test to the next. In particular, on the PMMA surface, we have noted a decrement of the SF corresponding to 40% from the first to the second test and to ~85% from the second to the third test. After the end of these three tests, the gecko could no longer stay attached with the hind feet. Figure 11 shows the negative effects of our seven consecutive tests, photographed 1 day after the first test-day subsequent to the second moult. A diffused inflammation of each gecko toe and the presence of small thin wound, located on the gecko skin between one toe and the next, were observed.

Regarding the self-renewal of the gecko adhesive system and abilities after the gecko's moulting process, we measured an increase of the gecko SF from $\lambda_{\text{Glass(I)-2Day}} \approx 0.5$ before the second moult to $\lambda_{\text{Glass(II)-1 Day}} = 9.13$ after the second moult. The increment of SF is also appreciable on the PMMA surface: from a SF $\lambda_{\text{PMMA(I)-3Day}} \approx 2.1$, before the second moult, up to $\lambda_{\text{PMMA(II)-1Day}} \approx 5.6$ after the second moult.

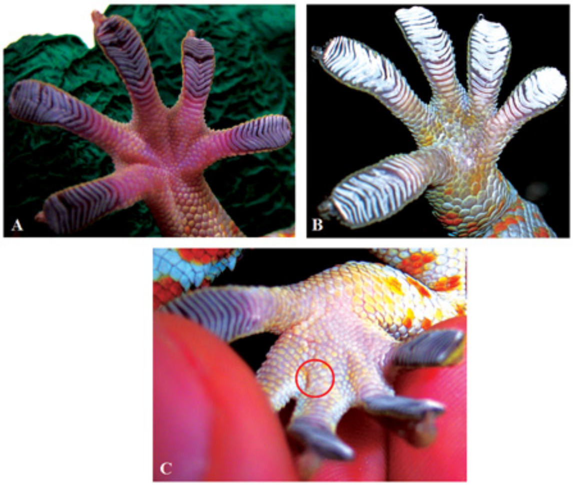

FIGURE 11 Damage on the feet imposed by the adhesive tests: (A) diffused inflammation of each gecko toe; (B) a healthy gecko foot is here reported for comparison; (C) small thin wound located on the gecko skin between one toe and the next (color figure available in online).

5. CONCLUSIONS

We have measured normal adhesive force-displacement curves of a live gecko. Thus, the gecko maximum SF was determined to be $\lambda_{\mathrm{PMMA}} = 10.23$ on the PMMA surface, that showed in general higher roughness and index S_{dr} (25 times greater than that of glass), and $\lambda_{\mathrm{Glass}} = 9.13$ on the glass surface. We observed a clear trend of the adhesion ability during the period after the moulting: normal adhesive forces drastically decrease at each subsequent test as a consequence of the damage of the gecko feet caused by our previously executed experimental tests. Finally, we documented the observed self-renewal of the gecko adhesive system and abilities after the moulting. The analysis here reported could have also implications in the design of bio-inspired smart adhesive materials.

ACKNOWLEDGMENTS

The authors would like to thank M. Nervo and M. Buono, DVM and SIVAE member, for the technical and veterinary aid. Also the authors are grateful to M. Biasotto of the Department of Special Surgery and F. Antoniolli of the Department of Biomedicine at the University of Trieste for their help in using the AFM. We gratefully acknowledge A. Chiodoni, Department of Physics, Politecnico of Torino, for the help in performing the FESEM micrographs. We thank the "2I3T Scarl – Incubatore dell'Università di Torino" for SEM imaging instruments and M.G. Faga, CNR-ISTEC member, Chemical Department IFM and NIS Centre of Excellence, University of Torino, for the help in performing the SEM micrographs. NMP is supported by "METROLOGY ON A CELLULAR AND MACROMOLECULAR SCALE FOR REGENERATIVE MEDICINE" – METREGEN (2009–2012).

REFERENCES

[1] Aristotle, *Historia Animalium*, 343 B.C. See Book IX, Part 9, translated by Thompson DAW, The history of animals, http://classics.mit.edu/Aristotle/history_anim.html last (accessed 26 Sep 2011).
[2] Irschick, D. J., Austin, C. C., Petren, K., Fisher, R. N., Losos, J. B., and Ellers, O., *Biol. J. Linn. Soc.* **59**, 21–35 (1996).
[3] Carrier, O., *Verhandl. Wurz Phys-med Gesell* **1**, 83–96 (1872).
[4] Haase, A., *Archiv. Naturgesch* **66**, 321–345 (1900).
[5] Gadow, H., *Amphibia and Reptiles*, (MacMillan and Co., Ltd., London, 1901).
[6] Weitlaner, F., *Verhdl. Zool. Bot. Ges. Wien.* **52**, 328–332 (1902).
[7] Schmidt, H. R., *Jena. Z. Naturwiss* **39**, 551–580 (1904).
[8] Hora, S. L., *J. Proc. Asiat. Soc. Beng.* **9**, 137–145 (1923).
[9] Dellit, W. D., *Jena. Z. Naturwiss* **68**, 613–658 (1934).

[10] Mahendra, B. C., *Proc. Indian. Acad. Sci.* **13**, 288–306 (1941).
[11] Maderson, P. F. A., *Nature* **203**, 780–781 (1964).
[12] Ruibla, R. and Ernst, V., *J. Morph.* **117**, 271–294 (1965).
[13] Hiller, U., *Z. Morphol. Tiere* **62**, 307–362 (1968).
[14] Hiller, U., *Forma et Functio.* **1**, 350–352 (1969).
[15] Gennaro, J. G. J., *Nat. Hist.* **78**, 36–43 (1969).
[16] Williams, E. E. and Peterson, J. A., *Science* **215**, 1509–1511 (1982).
[17] Stork, N. E., *J. Exp. Biol.* **88**, 91–107 (1980).
[18] Liang, Y. A., Autumn, K., Hsieh, S. T., Zesch, W., Chan, W. P., Fearing, R., Full, R. J., and Kenny, T. W., *Technical Digest of the 2000 Solid-State Sensor and Actuator Workshop* **200033**, 38 (2000).
[19] Autumn, K, Liang, Y. A., Hsieh, S. T., Zesch, W., Chan, W. P., Kenny, T. W., Fearing, R., and Full, R. J., *Nature* **405**, 681–685 (2000).
[20] Autumn, K., Ryan, M. J., and Wake, D. B., *Q. Rev. Biol.* **77**, 383–408 (2002).
[21] Tinkle, D. W., *Encyl. Amer. Grolier.* **12**, 359 (1992).
[22] Eisner, T. and Aneshansley, D. J., *Proc. Natl. Acad. Sci. USA* **97**, 6568–6573 (2000).
[23] Kesel, A. B., Martin, A., and Seidl, T., *J. Exp. Biol.* **206**, 2733–2738 (2003).
[24] Federle, W., Rohrseitz, K., and Hölldobler, B., *J. Exp. Biol.* **203**, 505–512 (2000).
[25] Walker, G., *Int. J. Adhes. Adhes.* **13**, 3–7 (1993).
[26] Pugno, N. M., *J. Phys.: Condens. Matter* **19**, 395001, 1–17 (2007).
[27] Autumn, K., Sitti, M., Liang, Y. A., Peattie, A. M., Hansen, W. R., Sponberg, S., Kenny, T. W., Fearing, R., Israelachvili, J. N., and Full, R. J., *Proc. Natl. Acad. Sci. USA* **99**, 12252–12256 (2002).
[28] Autumn, K. and Peattie, A. M., *Int. J. Comp. Biol.* **42**, 1081–1090 (2002).
[29] Huber, G., Gorb, S. N., Spolenak, R., and Arzt, E., *Biol. Lett.* **1**, 2–4 (2005).
[30] Huber, G., Gorb, S. N., Hosoda, N., Spolenak, R., and Arzt, E., *Ada. Biomater.* **3**, 607–610 (2007).
[31] Autumn, K., Dittmore, A., Santos, D., Spenko, M., and Cutkosky, M., *J. Exp. Bio.* **209**, 3569–3579 (2006).
[32] Huber, G., Mantz, H., Spolenak, R., Mecke, K., Jacobs, K., Gorb, S. N., and Arzt, E., *Proc. Natl. Acad. Sci. USA* **102**, 16293–16296 (2005).
[33] Autumn, K., Hsieh, S. T., Dudek, D. M., Chen, J., Chitaphan, C., and Full, R. J., *J. Exp. Bio.* **209**, 260–272 (2006).
[34] Schleich, H. H. and Kästle, W., *Amphib. Reptil.* **7**, 141–166 (1986).
[35] Lepore, E., Antoniolli, F., Brianza, S., Buono, M., Carpinteri, A., and Pugno, N., *J. Nanomat.* **194524**, 1–5 (2008).
[36] Pugno, N. and Lepore, E., *J. Adhesion* **89**, 949–962 (2008).
[37] Pugno, K. and Lepore, E., *Biosystems* **94**, 218–222 (2008).
[38] Pugno, N., *Nano Today* **3**, 35–41 (2008).
[39] Varenberg, M., Pugno, N., and Gorb, S., *Soft Matter* **6**, 3269–3272 (2010).
[40] Lepore, E., Chiodoni, A., and Pugno, N., *Rev. Adv. Mat. Sci.* **24**, 69–80 (2010).
[41] Buehler, M. J., Yao, H., Gao, H., and Ji, B., *Modelling. Simul. Mater. Sci. Eng.* **14**, 799–816 (2006).
[42] Keten, S., Xu, Z., Ihle, B., and Buehler, M. J., *Nature Materials* **9**, 359–367 (2010).
[43] Gorb, S., Gorb, E., and Kastner, V., *J. Exp. Bio.* **204**, 1421–1431 (2001).
[44] Buehler, M., *J. Nano Today* **5**, 379–383 (2010).